Jurnal Teknologi

Full Paper

COMPRESSED SYNTHETIC APERTURE RADAR IMAGING BASED ON MAXWELL EQUATION

Rahmat Arief[a,b*], Dodi Sudiana[a], Kalamullah Ramli[a]

[a]Department of Electrical Engineering, Universitas Indonesia
[b]Remote Sensing Division, Indonesian National Institute of Aeronautics and Space (LAPAN), Indonesia

Article history
Received
11 June 2015
Received in revised form
26 October 2015
Accepted
12 January 2016

*Corresponding author
rahmat.arief@ui.ac.id
rahmat.arief@lapan.go.id

Graphical abstract

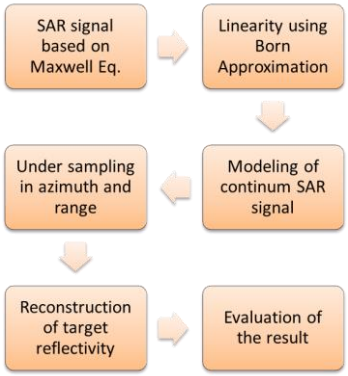

Abstract

Within few years backward, researches had presented the ability of compressive sensing to handle the large data problem on high resolution synthetic aperture radar (SAR) imaging. The main issue on CS framework that should be dealt with the SAR imaging is on the requirement of linearization on the measurement system. This paper proposes a new approach on formulating the compressed SAR echo imaging system which is derived from the Maxwell's equations with continuous signal along the SAR antenna movement. Born approximation is applied to approximate the linear form of the SAR echo imaging system. In addition, the compressed sampling is formed by reducing the sampling rate of received radar signals randomly simultaneously on both of low sampling of fast time and slow time signals and by reducing the pulse period interval of transmitted signals. The simulation's result shows that a better focused reconstructed sparse target can be achieved compared with the conventional match filter based Range Doppler (RD) method.

Keywords: Born approximation; compressive sensing; fast time and slow time sampling; Maxwell equation; Synthetic aperture rada

1.0 INTRODUCTION

SAR imaging is a technology to generate high resolution radar image in wide area [1], [2]. Some critical challenges in the SAR Technology [3], [4] are transmitting microwave energy at high power and detecting high rate received signal. The scattering signal from the target is carried by electromagnetic waves and received at the receiving antenna with a high sampling rate analog digital converter (ADC) which led to a large amount of data.

Compressive Sensing framework provides ability to reduce the energy by decreasing the transmitted signal randomly. In addition, it is also possible to reduce the load of a radar onboard system by using a low rate receiver system for receiving high rate radar signals. According to [5], [6], CS theory can recover specific signal by solving the linear optimization problem from fewer number of sampling than required under Nyquist/Shannon theorem. In other words, the high rate ADC on conventional system can be replaced with the low rate ADC. So that power and onboard components of a radar system can be reduced and the volume of data that contains SAR signal becomes small. By having those conditions, the quality of SAR imagery can still be maintained and even improved compared with conventional systems.

First crucial step on CS framework is to linearize the measurement system. Thus, the SAR signal measurement system should be approached by linearization. Several studies have addressed on a linear modeling of SAR signal i.e. Herman [7] proposed

a linear model of the SAR signal with Alltop-sequence models and Wei [8] derived SAR echo signal by separation of targets from SAR raw data.
Another approach of linear model of SAR raw data is derived from Maxwell equations [3], [4], [9]. Sun [9] proposed a model of SAR echo of Maxwell's equations in the frequency domain and compressive sampling matrix model which is constructed from random matrix Fourier partially on the direction of fast time to process the CS SAR imaging.

This paper proposed a new linear equations model of SAR signal in the function of slow time and fast time which is used to reconstruct the sparse target on CS-based SAR imaging.

The SAR signal equation is derived from Maxwell equation and formed into a linear equation using the Born approximation. Based on the linear equations model is defined a good compressed sampling simultaneously in both directions fast time and slow time in the time domain at random. To obtain the reconstructed target is used the L1-norm minimization [5], [6], [10].

2.0 SAR MODEL BASED ON MAXWELL EQUATION

2.1 EM Wave Propagation

SAR echo is generated from received EM waves at the antenna and used to form the SAR image. Almost all SAR imaging system using the Stop-Go approximation [11], in which the SAR sensor and the target are assumed at fixed position and time when the chirp pulse hit the target and back to the antenna. Energy source hits an object as incident field and it causes the radiation scattering from the object called scattered field. Overall electric field can be defined in two components as expressed

$$\mathcal{E}^{tot}(t,x) = \mathcal{E}^{in}(t,x) + \mathcal{E}^{sc}(t,x) \tag{1}$$

where $\mathcal{E}^{in}(t,x)$ is the incident field which is a model of the electric field of the signal transmitted from the antenna on the target and $\mathcal{E}^{sc}(t,x)$ is the scattered field which is a model of electric field of the signal from the target which is received by the antenna.
As observed in [3], [4], [9], the Maxwell's equations can be used to obtain a scalar EM wave equation of the SAR signal. Both incident field and scattered field can be formulated as scalar EM wave equation of the SAR signal in differential and integral form as follow :

$$\left(\nabla^2 - \frac{1}{c_0^2}\frac{\partial^2}{\partial t^2}\right)\mathcal{E}^{in}(t,x) = -j(t,x) \tag{2}$$

$$\mathcal{E}^{in}(t,x) = -\iint g(t-t',x-y)\, j(t',y)dtdy\,..$$

$$\left(\nabla^2 - \frac{1}{c_0^2}\frac{\partial^2}{\partial t^2}\right)\mathcal{E}^{sc}(t,x) = -V(x)\frac{\partial^2}{\partial t^2}\mathcal{E}^{tot}(t,x) \tag{3}$$

$$\mathcal{E}^{sc}(t,x) = -\iint g(t-t',x-z)\, V(z)\frac{\partial^2}{\partial t^2}\mathcal{E}^{tot}(t',z)\, dtdz\,..$$

When an incident field has contact to the object, it will induce currents hence the object emits the scattered field which is the same signal, but weaker and time delayed. The scattered field $\mathcal{E}^{sc}(t,x)$ is formed from the interaction between the target and the incident field $\mathcal{E}^{in}(t,x)$. Thus its value is the response target depends on the geometry and material properties of the target and of the shape.

The function $g(t,x)$ can be interpreted as the electric field at time t and position x of an electric field sources and called the outgoing fundamental solution or the (outgoing) Green function [12], [13]. The above problems of the constant-speed wave equation with a source of an antenna current density $j(t,x)$ can be solved by using the Green's function, then the new equations of scattered signal can be written as follows:

$$\mathcal{E}^{sc}(t,x) = -\iint \frac{\delta(t-|x-z|/c)}{4\pi|x-z|} V(z)\frac{\partial^2}{\partial t^2}\mathcal{E}^{tot}(t',z)dt\, dz \tag{4}$$

The equation (4) is integral Lippman-Schwinger equation which shows that $\mathcal{E}^{sc}$ depends on the total electric field. The equation becomes non linear, because $\mathcal{E}^{sc}$ exist on both sides of the equation. This has consequences that $\mathcal{E}^{sc}$ becomes complex to be resolved.

2.2 Born Approximation

For radar imaging, the scattered field can be measured at the antenna and the reflectivity V(z) is a function that must be resolved. By the non-linear equation on (4) the reflectivity function will be hard to be solved. Thus, Born approximation (weak scattering approximation) is applied to approach the solution. $\mathcal{E}^{sc}$ is assumed to be much weaker than the incident field $\mathcal{E}^{in}$ ($\mathcal{E}^{sc} \ll \mathcal{E}^{in}$). So that $\mathcal{E}^{tot}$ on the right side of the equation is replaced by $\mathcal{E}^{in}$ in ($\mathcal{E}^{in} \approx \mathcal{E}^{tot}$). The new equation of scattered field can be derived as :

$$\mathcal{E}_B^{sc}(t,x) = -\iint \frac{\delta(t-|x-z|/c)}{4\pi|x-z|} V(z)\frac{\partial^2}{\partial t^2}\mathcal{E}^{in}(t',z)\, dt\, dz. \tag{5}$$

where $t' = |x-z|/c$ is the time of the EM wave needed to cover the distance between the antenna and the target. The scattered field equations in frequency domain are written as follow

$$E_B^{sc}(\omega,x) = -\int_z \frac{e^{-ik|x-z|}}{4\pi|x-z|} V(z)\,\omega^2\, E^{in}(\omega,x)\, dz \tag{6}$$

where $J(\omega,y)$ is the current source and $V(z)$is the reflectifity factor in the frequency domain. Born approximation is very useful to linearize the equation of radar signals. The approach to this method is not necessarily the best do to in fact some artifacts are ignored in the radar imaging.

3.0 MODEL OF SAR SIGNAL SCATTERING MATRIX

3.1 Incident Field

As observed in [3], [9], the antenna current density will be modeled such that $j(t,x) = p(t)\delta(x-y)$ at the antenna position y and p(t) is the transmit signal on the antenna. The transmitted signal is considered in the form of a linear chirp (frequency modulated pulse) with the carrier frequency f_0.

$$p(t) = G_a \cdot a(t) \cdot e^{i(\omega_0 t + \pi\alpha t^2)} \quad (7)$$

where G_a is an amplitude function independent to the transmitted signal which can be a constant value or varies for a wideband signal even within a short pulse time duration. $a(t)$ represents a rectangular function. The carrier frequency is related to the angular frequency $\omega_0 = 2\pi f_0$, $\alpha = B/2T_p$ is the chirp rate, T_p is pulse duration, and B is the bandwidth of the chirp signal. In the frequency domain, the corresponding source is $J(\omega,x) = P(\omega)\delta(x-y)$, where $P(\omega)$ is the Fourier transform of $p(t)$.

3.2 Continum Model of SAR Echo

The incident electric field is generated in the frequency domain is as follows:

$$E^{in}(\omega,x) = -\frac{e^{-ik|x-z|}}{4\pi|x-z|} P(\omega) \quad (8)$$

The scattered field based on Born approximation is generated by substitution Eq. (6) and Eq. (8), so that we get the measured data as follow

$$E^{sc}(\omega,x') = \int_z \frac{e^{-ik|x-z|}}{4\pi|x-z|} V(z)\, \omega^2 \frac{e^{-ik|y-z|}}{4\pi|y-z|} P(\omega)\, dz \quad (9)$$

It is assumed a monostatic case, where the position of the transmitting antenna x and receiving antenna y are in one platform (x=y) and the distance between the target position z from the antenna x and y is far. Then scattered field by the receiving antenna is obtained as follows

$$\mathcal{E}^{sc}(t,x) = -\int \frac{\omega_0^2}{16\pi^2 R^2} V(z).a(t).G_a\, e^{i(\omega_0(t-\tau)+\pi\alpha(t-\tau)^2)} dz \quad (10)$$

where $R(z) = |x-z|$ is the distance between the antenna and the target and $\tau = 2R(z)/c$ is the time delay, which is the travel time of chirp signal from the antenna to the target and back to the antenna.

A base band modulated signal can be obtained by eliminating the carrier frequency, followed by a lowpass filter through quadrature demodulation process is as follows:

$$\mathcal{E}_B^{sc}(t,x) = -\int \frac{\omega_0^2}{16\pi^2 R^2} V(z).a(t).G_a.\, e^{(-i\omega_0\tau + i\pi\alpha(t-\tau)^2)} dz \quad (11)$$

The above formula applies to the pulse radar system based on stop-go approximation [11], which is the transmit signals is sent at an certain antenna position x and time t. In continuum model, radar antenna is usually pointed toward the earth on the moving platform and simultaneously emits radar signals. The antenna path is denoted by index η_i, which represents antenna position movement path with $\eta_i = 1, \ldots, N$. The time scale on this model is defined into 2 scales, which the time scale on the antenna movement is much slower (slow time) than the time scale on the EM wave of a radar signal (fast time). Then the received radar signal can be defined as follows:

$$\mathcal{E}_B^{sc}(t,\eta_i) = -\int \frac{\omega_0^2}{16\pi^2 R_{\eta_i k}^2} V(z).a(t).G_a.\, e^{\left(-i\omega_0\tau_{\eta_i k} + i\pi\alpha\left(t-\tau_{\eta_i k}\right)^2\right)} dz \quad (12)$$

where $\tau_{\eta_i k} = 2.R_{\eta_i k}/c$ is the delay time of SAR echo at index η_i dan $R_{\eta_i k}$ is the distance (range) between the radar antenna at the position η_i and each target at the position $z(x_k, y_k)$. The distance is formulated as follow

$$R_{\eta_i k} = \sqrt{(\eta_i^2 - y_k^2) + (h^2 + (X_c + x_k)^2)} \quad (13)$$

where h is height of the radar sensor and X_c is the range center to target.

4.0 COMPRESSED SAR

4.1 Linear Model Model Of SAR Signal

The goal of SAR image reconstruction is to determine the target reflectivity V_k from the mesured SAR echo $\mathcal{E}_B^{sc}(t,\eta_i)$. The SAR echo may not have sparse properties in one domain, but the scene could be sparse in different domain. The simplest form of sparsity in the SAR imaging would be a scene containing of a few numbers of dominant scatterers e.g. ships at ocean. As assumed, $V_k \in \mathbb{C}^{Nx1}$ is scattering coefficients which indicate the magnitude of target reflectivity in complex signal, which has a small number of K non-zeros dominant scatterers in a vector length N.

A linear model of SAR echo is reconstructed from Eq. (12) in a discrete form as follow

$$s_{RT}(t_n,\eta_i) = \sum_{k=1}^{N} \psi_k(t_n,\eta_i).V_k \quad or \quad S = \Psi.V_k \quad (14)$$

The time scale of fast time and slow time signal is indexed by $t_n = 1, \ldots, N_r$ and $\eta_i = 1, \ldots, N_a$ where N_r and N_a are the amount of sampling number of fast time and slow time signal. The vektor $\psi_k(t_n,\eta_i)$ for each target can be constructed as

$$\psi_k(t_n,\eta_i) = A_k.e^{-j\varphi(t_n,\eta_i)} \quad (15)$$

$$\psi_k(t_n,\eta_i) = [A_k e^{-j\varphi_1(1,1)}, \ldots, A_k e^{-j\varphi_1(1,N_r)}, A_k e^{-j\varphi_1(2,1)}, \ldots, A_k e^{-j\varphi_1(N_a,N_r)}]^T$$

where $A_k = \frac{\omega_0^2}{16\pi^2 R_{\eta_i k}^2} \left|a\left(t_n - \frac{2R_{\eta_i k}}{c}\right)\right|^2 .G_a$

$$\varphi(t_n, \eta_i) = 4\pi f_c \frac{R_{\eta_i k}}{c} - \pi K_r \left(t_n - \frac{2R_{\eta_i k}}{c}\right)^2$$

Suppose the scatter coefficients vector $\mathrm{V_k} = [\mathrm{v_1}, \mathrm{v_2}, \cdots, \mathrm{v_N}]^{\mathrm{T}}$, the new mathematical model of general SAR signal acquisition Ψ is interpreted as basis vector at the fast-time t_n and slow-time η_i and can be written as

$$\Psi = [\psi_1(t_n, \eta_i), \psi_2(t_n, \eta_i), \ldots, \psi_N(t_n, \eta_i)] \quad (16)$$

The matrix Ψ has dimension of $\mathrm{N_a N_r} \times \mathrm{N_{target}}$. A digital SAR raw data is obtained by using high rate analog digital converter (ADC) as required by the Nyquist theorem.

In many cases the radar scene is sparse in the sense that only a small fraction of the cells is occupied by the objects of interest. Thus, the target reflectivity $\mathrm{V_k}$ consist few of strong scatterers around the weak backscatter area. It shows bright objects in the SAR image. The bright objects often related to man-made structures or vehicles are typically sparse in the space domain, i.e. several ships at sea. The metal feature has strong scatterers and sea is weak scatterer.

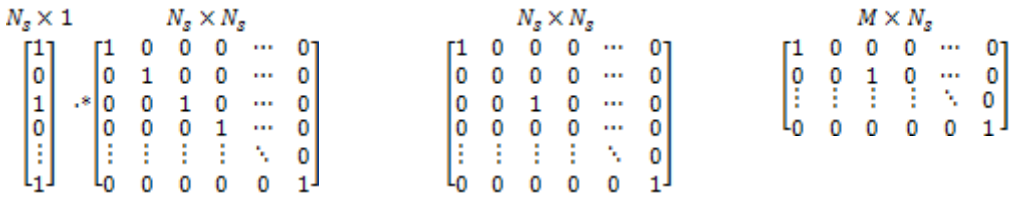

Figure 1 Generation of sampling matrix Φ

According to CS theory, it is possible to recover the sparse signal from a very few of samples of the signal than required under Nyquist/Shannon theorem.

4.2 Model of Compressed Sampling

In order to show the effectiveness of recovery performance from CS algorithms on a sparse SAR scene, a few of random measurement of received SAR signal $\mathrm{S_{RT}}$ is needed. Given the measurement y, the reconstruction of a sparse scene $\mathrm{V_k}$ is obtained such that

$$y = \Phi S_{RT} = \Phi \Psi V_k + n \quad (17)$$

where measurement matrix Φ denotes a $\mathrm{M} \times \mathrm{N_s}$ $(N_s = N_a N_r)$ matrix which is constructed randomly. The number of measurements M must be selected at least greater than K but can be significantly smaller than the scene dimension $\mathrm{N_s}$ $(\mathrm{K} < M \ll \mathrm{N_s})$.

The SAR image is formed from each backscattered signal in the fast time and in the slow time direction. The under sampling is conducted by reducing the measurement amounts of received radar signals randomly simultaneously in the both of fast time and slow time signals. They are (1) under sampling in slow time which is generated by randomly selection of transmitted radar pulses. (2) under sampling in fast time which is generated by receiving fewer randomly selected backscattered signal than conventional Nyquist sampled system.

Figure 1 describes generation of sampling matrix Φ. The reduced measurements are conducted by binary randomly under sampling of the radar signal based on the identity matrix. The identity matrix which has size $\mathrm{N_s} \times \mathrm{N_s}$ of is multiplied by a binary random permutation array. Then The final compressed sampling matrix can be formed by removing the row with value 0 and has size of $M \times \mathrm{N_s}$ .This method shows decreasing of the number of samples significantly.

4.3 Reconstruction

To find the approximation of sparse SAR scene from a few of random samples number of SAR raw data can be done by solving the inverse problem using the L1 minimization [6], [10].

$$\hat{V}_k = arg\ min \| y - \Phi \Psi V_k \|_1 < \varepsilon \quad (18)$$

where ε is amount of energy of the error. The choice of ε is dedicated by type of the errors and can be estimated from measured echo signal.

The algorithms can be seen as an attempt to exploit the sparsity or compressibility of the scene reflectivity by solving an inverse problem either through a linear program

5.0 RESULTS AND DISCUSSION

This section evaluates the performance of compressed SAR imaging derived for the Maxwell equation. Some experiments on two SAR scenes, i.e target points and a complex object of ship are conducted to evaluate the proposed method. The scenes are selected targets from a two-dimensional target profile of reflectivity over the azimuth and range based on the intensity of the pixels in the target image (see Figure 2).

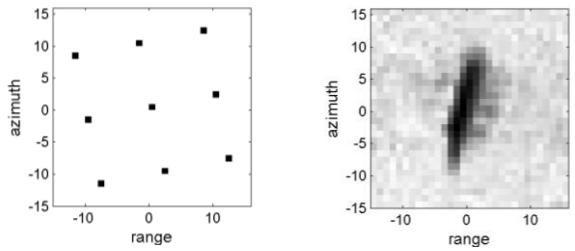

(a) (b)

Figure 2 Input SAR scenes of (a) points target and (b) a complex object of a ship image

Both target scenes consist points or object with different scattering response in a 31x31 pixel image. The important parameters of SAR stripmap mode are 10 GHz frequency center with 1.00 m of azimuth and range resolution respectively. SAR raw echo is acquired with sampling rate as required by the Nyquist theorem. We obtained the size of SAR raw echo $Na \times Nr$, which means the maximum number of samples in azimuth (slow time) and range (fast time) axis $\mathbf{N_a = 96}$ and $\mathbf{N_r = 126}$ respectively. Under sampling measurement of the SAR raw echo is conducted to reduce the SAR raw echo.

5.1 Experiments Using Point Target

In the first experiment, the input SAR scene of point target is used. Random measurements were conducted as compressed sampling M=50-100 samples simultaneously in the both azimuth and range. Thus the overall amount of random sampling under 1% samples of the total number of sampling $Ns = Na * Nr$=12096. The amount of under sampling measurements is taken arround the requirement of the RIP in order to ensure good reconstruction. To gain the stable final result, the calculations of the reconstructed result are conducted repeatedly100 times.

Measuring the quality of the reconstruction results is conducted using 2 criterions: (a) the quality of the image that is marked with pseudo signal noise ratio (PSNR) and the root mean square error (RMSE) values [14], (b) the quality of SAR image which is determined by the value of the image resolution in 3dB resolution, the peak side lobe ratio (PSLR) and the integrated side lobe ratio (ISLR) on the spectrum of point spread function in range and azimuth axis[15]. Image resolution of SAR is defined by width of the main lobe of the impulse response measured 3 dB below the peak value. PSLR and ISLR represent the ability of the SAR to identify a strong target from nearby weak targets. PSLR and ISLR are the ratio between the height of the main lobe and the side lobe, expressed in decibels (dB).

Figure 3 shows the imaging results of the point targets using both MF-based RD algorithm [1] and the presented CS method respectively. The results of RD algorithm for the scene are shown in Figure 3(a). There is serious side lobe interference in the imaging results using RD algorithm. Solving the convex optimization problem using presented method, the results using only M=60-100 random samples are shown in Figure 3(b)-(f). It is showed that the target positions and amplitudes of point targets are significantly reconstructed compared with the RD algorithm by M≥60. Contrarily, the point targets cannot be reconstructed properly, if the SAR echo is randomly sampled by the number of measurements under M = 50.

The performance of CS relies on the number of measurements. The larger the number of echo samples are, the more scattering centers can be reconstructed.

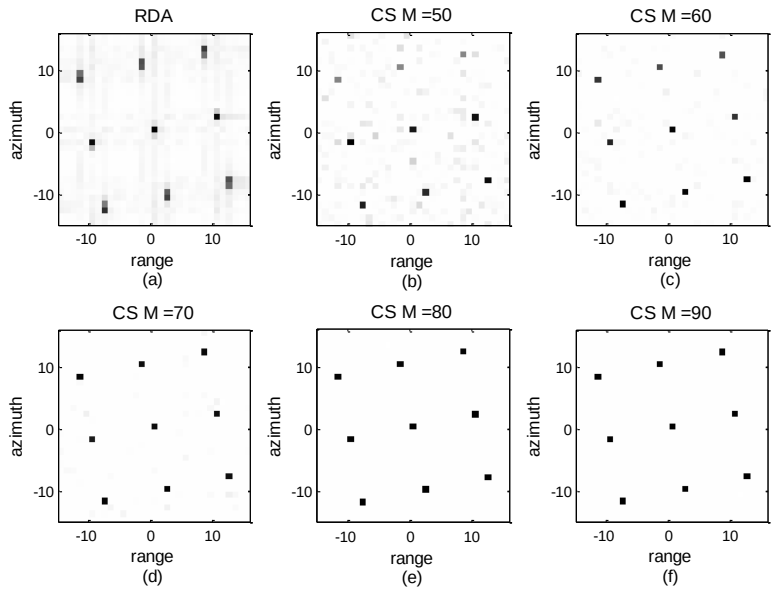

Figure 3 Reconstruction results of approximated point targets scenes using (a) RDA (b)-(f) SAR based CS processing with different amount of measurement from M=50 – 90

Table 1 The quantitative results based on SAR image quality parameter of approximated point target using RDA processing and CS based SAR processing with different amount of measurement number

	Comp. Ratio M/N[%]	PSNR [dB]	RMSE	Range			Azimuth		
				3dBmw [m]	PSLR [dB]	ISLR [dB]	3dBmw [m]	PSLR [dB]	ISLR [dB]
RDA	100	23,206	0,203	1,25	-7,014	-8,402	1,06	-11,151	-7,593
CS M=50	0,413	24,682	0,589	1,00	-7,153	-8,859	1,02	-10,113	-10,342
CS M=60	0,496	32,293	0,241	1,00	-15,214	-10,786	1,00	-13,514	-10,834
CS M=70	0,579	42,173	0,063	1,00	-17,610	-10,939	1,00	-27,550	-10,960
CS M=80	0,661	53,347	0,022	1,00	-27,813	-10,960	1,00	-30,030	-10,961
CS M=90	0,744	58,883	0,012	1,00	-30,167	-10,959	1,00	-34,721	-10,957
CS M=100	0,827	65,094	0,005	1,00	-31,920	-10,958	1,00	-35,833	-10,962

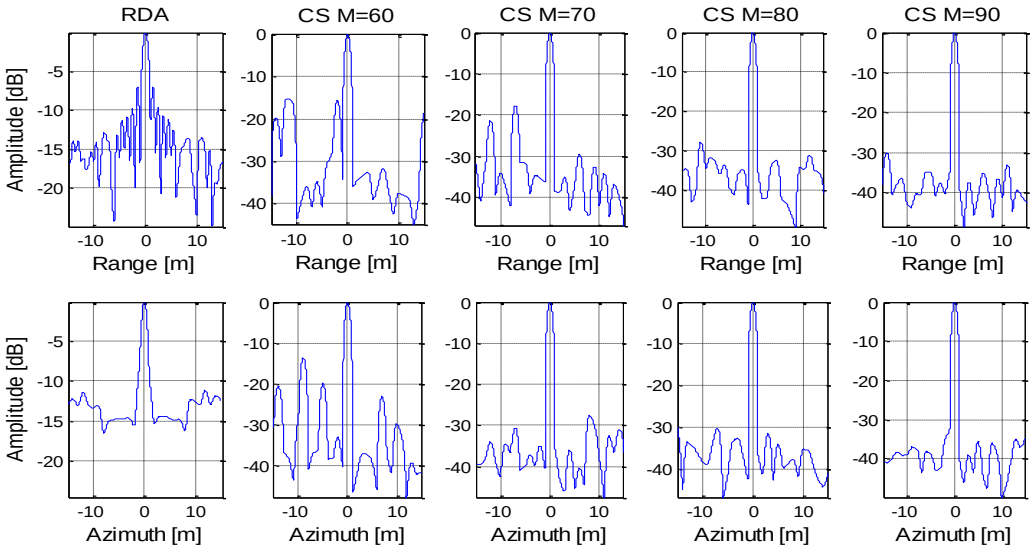

Figure 4 Spectrum of point spread function in range and azimuth of RDA processing and CS based SAR processing with amount of measurement number M=60-90

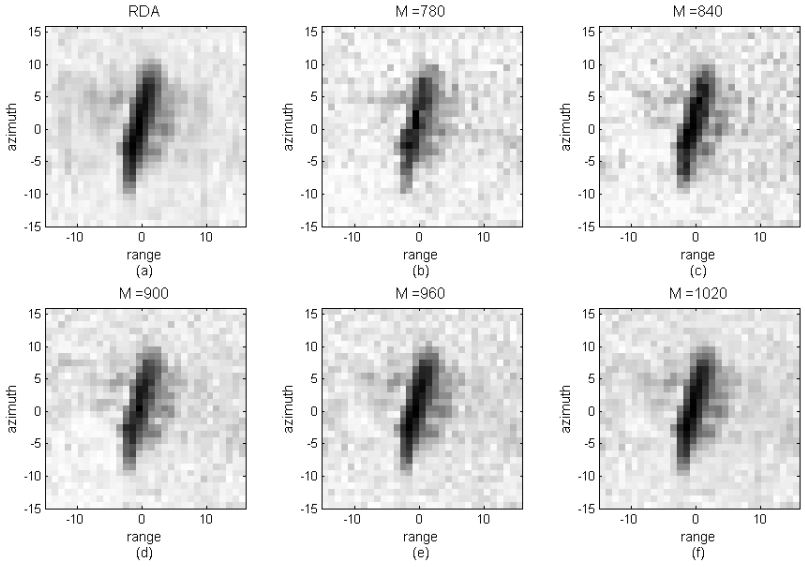

Figure 5 The imaging results of the ship scene by (a) RD algorithm, (b)-(f) the presented CS method with M=780-1020

Table 2 The quantitative results of the approximated scenes from a complex object of a ship using RDA processing and CS based SAR processing with different amount of measurement number

	Compression Ratio M/N [%]	PSNR [dB]	RMSE
RDA	100	26,6729	0,0463
CS M=840	6,94	24,1671	0,0620
CS M=870	7,19	24,9882	0,0563
CS M=900	7,44	26,7983	0,0458
CS M=930	7,69	27,3240	0,0430
CS M=960	7,94	31,6616	0,0261
CS M=990	8,18	35,1881	0,0174
CS M=1020	8,43	147,3641	4,27E-08

Performance of the reconstructed result using CS-based SAR processing can be measured by the values of PSNR and RMSE from the perspective of an image. Table 1 shows that the performance of the approximated scenes using CS-based SAR processing is improved. This is characterized by the higher value of PSNR and the smaller value of RMSE while increasing the number of measurements M. The imaging results using RDA have PSNR value of 23,206 dB adn RMSE value of 0,203, while the imaging results by using CS based SAR processing by M=60 and above show higher PSNR and smaller RMSE.

Moreover, the value of the side lobe in the presented method is significantly less than that in RD algorithm. While the value of PSLR of point target using RDA method are -7,014dB in range axis and -11,151 dB in azimuth axis, for point target using CS proposed method with M=60 the value of PSLR are -15,214 dB in range and -13,514 dB in azimuth. The variation of the side lobes of back scattered signal is reduced by increasing the amount of under sampling measurements. The value of 3dB resolution, PSLR and ISLR in both azimuth and range direction as a whole has slightly improved (see table 1).

5.2 Experiments Using A Complex Object Of A Ship

The original ship image from Radarsat1 is shown in figure 2(b). For conventional method, the radar raw data were full sampled according of Shannon /Nyquist theorem. And the SAR target of ship was reconstructed based on match filter processing algorithm (range doppler algorithm), which is most used SAR image formation algorithm today.

The number of random measurements were selected M=840-1020 samples or 6,94% - 8,43% of full raw data simultaneously in the both azimuth and range.

Figure 5 shows the imaging results and the evaluation performance of proposed method on the complex object of a ship compared with the conventional match filter based algorithm (RDA). Compared with the RDA, the presented CS method can significantly improve the imaging resolution of SAR by increasing the number of measurement M≥900.

The table 2 shows the quantitative performance of the approximated scenes in form of PSNR and RMSE and the compression ratio. With randomly subsampled data, the CS-proposed system can slightly recover the ship scene as performed as the RDA at only M=900 or 7.44 % of full raw data with PSNR of 26,7983 dB and RMSE of 0,0458. High recovery rates can even be achieved when only a small percentage starting from 7.44 % of raw data is available.

The results show that for the considered scenario, the locations and scattering coefficients of ship scene are well extracted by CS method. Thus SAR images reconstructed by the CS-proposed system lead to better quality than that of the RDA based recovered SAR images.

6.0 CONCLUSION

This paper presents a method of compressed SAR imaging based on compressive sensing which is derived from Maxwell's equation. Born approximation is applied to approximate the linear form of the SAR echo imaging system.

Due to this linearity, the CS theory possible to be used as one of solution tools to reconstruct sparse targets by solving the convex linear problem from fewer measurements than Nyquist theorem required.

Based on simulation's result, the proposed method significantly suppresses the side lobe and improves the imaging performance of the SAR significantly compared with conventional RD imaging method. The sampling rate at SAR signal can be drastically reduced. However, there are still some challenges to overcome in SAR imaging based on CS.

Acknowledgements

The authors would like to thank Mahdi Kartasasmita for many valuable comments and suggestions which significantly improved this paper.

References

[1] Cumming G. and Wong F. H. 2005. *Digital Processing of Synthetic Aperture Radar Data*. Norwood, MA: Artech House.
[2] Curlander J. C.and McDonough R. N. 1991. *Synthetic Aperture Radar: Systems and Signal Processing*. New York, John Wiley & Sons.
[3] Cheney M. and Borden B. 2009. *Fundamentals of Radar Imaging*. Society for Industrial and Applied Mathematics.
[4] Cheney M. and Borden B. 2009. Problems in synthetic-aperture radar imaging. *Inverse Problems*. 25(12): 123005.
[5] Candes E. J.and Tao T. 2006. Near-optimal signal recovery from random projections: Universal encoding strategies?. *IEEE Transactions on Information Theory*. 52(12): 5406–5425.
[6] Donoho D. L. 2006. Compressed Sensing. *IEEE Transactions on Information Theory*. 52(4): 1289–1306.
[7] Herman M. A.and Strohmer T. 2009. High-Resolution Radar via Compressed Sensing, *IEEE Trans. Signal Process*. 57(6): 2275–2284.
[8] Wei S.-J., Zhang X.-L., Shi, J. and Xiang G. 2010. Sparse Reconstruction for SAR Imaging Based on Compressed Sensing. *Progress In Electromagnetics Research*. 109: 63–81.
[9] Sun B., Cao Y., Chen J., Li C., and Qiao Z. 2014. Compressive Sensing Imaging For General Synthetic Aperture Radar Echo Model Based on Maxwell's equations, *EURASIP Journal on Advances in Signal Processing*. 2014(1): 1-6.
[10] Victoria Stodden David Donoho Y. T. 1999. SparseLab, http://sparselab.stanford.edu/. Stanford University, 2010.
[11] G. Franceschetti and R. Lanari, *Synthetic Aperture Radar Processing*. Taylor & Francis.
[12] Friedlander F. G. and Joshi M. S. 1998. *Introduction to the Theory of Distributions*. Cambridge University Press.
[13] Treves F. 1975. *Basic Linear Partial Differntial Equations*
[14] Gonzalez R. C. and Woods R. E. 2006. *Digital Image Processing (3rd Edition)*. Upper Saddle River, NJ, USA: Prentice-Hall, Inc.
[15] Martinez A. and Marchand J. 1993. SAR Image Quality Assessment, *Revista de teledeteccion: Revista de la Asociacion Espanola de Teledeteccion*. 2(2): 1-5.